ACS APPLIED MATERIALS & INTERFACES

Research Article

Cite This: ACS Appl. Mater. Interfaces 2019, 11, 8685−8692

www.acsami.org

Magnetic Liquid Metals Manipulated in the Three-Dimensional Free Space

Liang Hu,*[,†,‡] Hongzhang Wang,[§] Xiaofei Wang,[†,‡] Xiao Liu,[‡] Jiarui Guo,[†,‡] and Jing Liu*[,§,∥]

[†]Beijing Advanced Innovation Center for Biomedical Engineering and [‡]School of Biological Science and Medical Engineering, Beihang University, Beijing 100083, China

[§]Department of Biomedical Engineering, School of Medicine, Tsinghua University, Beijing 100084, China

[∥]Beijing Key Lab of Cryo-Biomedical Engineering and Key Lab of Cryogenics, Technical Institute of Physics and Chemistry, Chinese Academy of Sciences, Beijing 100190, China

Supporting Information

ABSTRACT: In the present study, a magnetic liquid metal droplet (MLMD), which can be stretched in large scales both horizontally and vertically in the free space, is introduced. This MLMD is fabricated based on a multimaterial system including liquid metals, iron particles, and electrolytes. Such remarkable stretching capacity is reversible, long-lasting, and can be repeated for multiple times. The seemingly contrary properties, the good stretchability and the mechanic strength for three-dimensional (3D) stretch, should owe to the surface oxide over the MLMD. On the basis of the 3D stretching ability of the MLMD, an intelligent scalable conductor was achieved, which can make electrical connections at various directions in the 3D free space. Moreover, the vertically stretched MLMD can move horizontally with its half body in the solution and the other half in the air, which resembles the nature of an upright walking amphibian. All the behaviors can be precisely, conveniently, and contactlessly controlled by the magnetic field provided by permanent magnets. With all the appealing properties, this MLMD presents a fundamental and promising platform for the liquid metals to further develop the multi-freedom actuation in free space and eventually lead to the dynamically reconfigurable intelligent and biomimetic soft robots in the future.

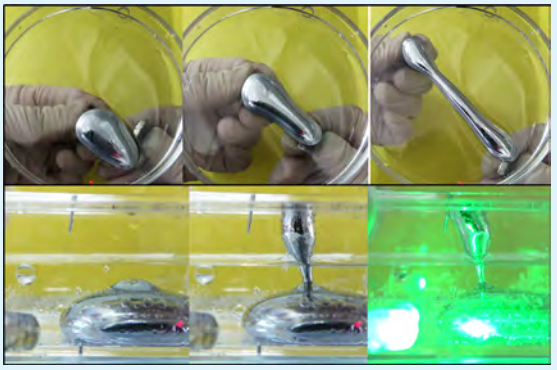

KEYWORDS: *magnetic liquid metals, 3D stretching, surface oxide, intelligent scalable conductor, soft robots*

INTRODUCTION

Room-temperature liquid metals (LMs) including gallium and eutectic alloys EGaIn or Galinstan in different proportions have drawn considerable attention in diverse applications. The unique and desirable properties such as high conductivity, low melting point, high deformability, and low toxicity are especially favorable in soft robots or machines and flexible electronics. The deformability and mobility of liquid metal objects in aqueous environments have been investigated extensively recently. In these studies, liquid metals have been manipulated by multiple means to achieve various functions such as soft pump,[1,2] electric switch,[3,4] motors,[5] or actuators.[6,7] In the design of these devices, the liquid metals usually have to be assembled in specific-designed microfluidic channels[3,8] or containers[1,4] to perform their functions. Besides, the liquid metals usually have to be immersed in alkaline or acidic solutions to prevent failures of the function because of the liquid metal surface oxidation. These restrictions limit the application of LMs in general circumstances such as in the free open space and in the air.

For soft robots or devices in the macroscopic scale, the abilities to deform, move, and function in the free space are of no doubt desirable and expected. This expectation can be also seen in science fiction films such as the Hollywood blockbuster Terminator, in which a pool of liquid metal can stand up and transform into a humanoid liquid metal robot with super-powers. As liquid metals have many unique properties promising for a future soft robot, considerable efforts have been made in the exploration of liquid metal actuation by noncontact approaches. However, it is still a challenge to manipulate the liquid metal in the three-dimensional free space because of its high density. For example, liquid metals have been reported to be driven by multiple approaches such as electric field,[9,10] magnetic field,[3,11] chemical,[12] electrochemical reactions,[5,8] light,[13] biomolecules,[14] and so forth. Because of the high surface tension, the LM droplets usually move as a whole droplet in the open space in these studies. Moreover, the

Received: January 3, 2019
Accepted: February 5, 2019
Published: February 15, 2019

DOI: 10.1021/acsami.8b22699
ACS Appl. Mater. Interfaces 2019, 11, 8685−8692

motion and transformation of these macro LM droplets are mostly on the approximate horizontal plane because of the large gravity. It is reported on the graphite substrate in the basic solution that the LM droplets can be propelled upslope.[15] However, the slope is quite gentle (<20°), and the vertical stretch or actuation in a large scale has still not achieved. Recently, alternating magnetic field (AMF) was used to successfully manipulate the pure LM in three dimensions.[16] However, the LM can be chemically unstable or even burned up because of rapid heating up under the high-powered AMF. Thus, the stand-up of the LM is transient and unsustainable, which may limit its further applications.

Magnetic control is a favorable driving option for soft robots because of its convenience, noncontact, and wireless properties. Permanent magnets can provide an intense magnetic field in a convenient and safe way, which is another feasible and valuable approach for manipulation of magnetic materials. Magnetic LMs have been reported to be fabricated by loading various magnetic nano/microparticles into LMs such as nickel,[17−19] iron,[3,20,21] gadolinium,[22] and so on. When directly exposed to the air, those magnetic LMs appear like paste because of severe oxidation. However, the high electrical conductivity still remains. Thus, they were often used as conductive paste to fabricate electronic circuits by 2D or 3D printing.[18,19,27]For magnetic liquid metals immersed in the solution such as HCl or NaOH, the interactions among the LM, the magnetic particles, and the solution become more complex. As the HCl/NaOH has the ability to dissolve gallium oxide, the LM droplet can generally remain a liquid state. Such magnetic liquid metals may provide a strategy for magnetic-driven soft LM-based devices or robot design. For example, the magnetic LM droplet can be manipulated in the microfluidic channel to perform their functions such as electric switches.[3,20] For the freely movable magnetic droplets, they were designed as motors for drug delivery.[11] However, for all these magnetic LM droplets, their locomotion driven by magnetic field is generally in the horizontal level because of the large gravity, which may limit their further applications in the three-dimensional space. Moreover, in the free open space, especially in the three dimensions, the stable and continuous manipulation of functional magnetic LM droplets is rarely reported.

In this study, a magnetic LM droplet (MLMD) with the ability of moving and stretching in a controllable and sustainable way in the open space is introduced. More intriguingly, this MLMD can even stretch and move in both horizontal and vertical direction. The standing-up and movable behaviors in the vertical direction remind us the liquid metal robot in the movie Terminator. Most surprisingly, this magnetic LM droplet can be manipulated with its half body in the liquids and other half in the air, which closely resembles the nature of an upright walking amphibian. With those and intriguing appealing properties, this MLMD presents great potential for further development of liquid metal-based soft robots. The detailed experiments and results are discussed as below.

RESULTS AND DISCUSSION

The MLMD was fabricated as illustrated in Figure 1a. Briefly, a liquid metal droplet (2 mL) was immersed in 2 mol/L HCl solution. Then, 4 g of iron (Fe) particles (~50 μm in diameter) was added in the solution. The LM was gradually mixed with iron particles by gentle stirring at room

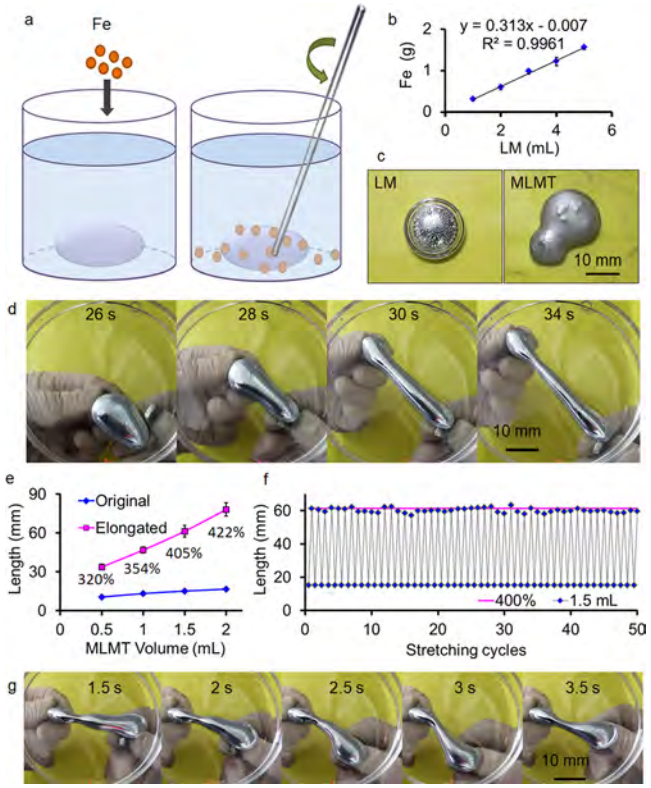

Figure 1. Magnetic liquid metal droplet. (a) The schematic illustration of MLMD preparation. (b) The absorption rate of iron (Fe) particles in liquid metals. (c) In 2 mol/L HCl, the LM remained a spherical shape with a bright metallic color, whereas the MLMD appeared dim and gray in an irregular shape. (d) The sequential snapshots of the stretching behavior of MLMD under the magnetic manipulation in the horizontal level. (e) The stretching ability of MLMD at various sizes (0.5−2 mL). The blue rhombuses indicate the diameter of the MLMD as a droplet at the original state. The pink squares indicate the elongated length of the MLMD as the long stick. The mean tensile range for each droplet size is also marked aside. (f) The MLMD (1.5 mL) can be stretched 50 times. The blue rhombuses indicate the MLMD length measured at the stretched and contracted states at each cycle. The pink line indicates a tensile range at 400%. (g) Local part of a stretching MLMD can be manipulated by the magnetic field.

temperature for around 3 min. The iron particles can be easily absorbed in the LM. Then, the LM droplet became magnetic because of the magnetism of iron particles. The absorption rate of iron was evaluated by weighting the LM droplet. On the basis of the results, around 0.31 g of iron particles was absorbed in every 1 mL of LM (around 6.05 g) by this means (Figure 1b). At the same time, it was observed that the LM droplet was covered with a dark oxide layer as well as redundant black iron particles as the Fe particles can easily attached to the gel-like tacky oxide surface. At the same time, the droplet did not maintain the spherical shape anymore (Figure 1c). We have also tried iron nanoparticles in preliminary studies. However, most of them quickly reacted with HCl before fully interacting with the LMs. The abundant hydrogen generation also interfered this interaction. After iron particles were fully absorbed, the droplet was transferred into other clean HCl solution for magnetic manipulation.

All the magnetic fields in this study are provided by neodymium−iron−boron magnets (NdFeB, 11 × 17.5 × 4 mm for one piece). When applying a single magnet under the

DOI: 10.1021/acsami.8b22699
ACS Appl. Mater. Interfaces 2019, 11, 8685−8692

whole droplet at a distance of 2 to 3 mm, the LM droplet can move with the magnet, which has also been reported in other studies. When applying two magnets in the opposite directions, the generally round MLMD can be elongated into a long thin stick (Figure 1d and Movie S1 in Supporting Information). For instance, a magnetic LM droplet with a diameter of 13.2 mm can be stretched into as long as 46 mm. The stretching ability of MLMD at various sizes was also evaluated. The results in Figure 1e suggest that the MLMD at large size has a large tensile range, which indicates better stretching ability. The tensile range can easily reach 400% when droplet volume is over 1.5 mL. This stretch can be also reversible by magnetic manipulation (Figure 1f and Movie S2 in Supporting Information). The process can be repeated over 100 times. Moreover, the elongated part can even make turns under the control of the magnetic field (Figure 1g and Movie S3 in Supporting Information), which presents great resemblance to a snake.

Such large deformation and elongation of the LM droplet in HCl solution are remarkable. The LM droplets usually maintain a spherical shape with high surface tension in the acid solution because the acid can dissolve surface oxide.[23] In the present study, obvious oxide layer formed on the LM droplet surface even in as high as 2 mol/L HCl. It is supposed that the key factor of such large deformation of the LM droplet should be the surface oxide, which can improve the deformability of the droplet by significantly reducing the surface tension. To prove this assumption, the relation between the surface tension and its deformability was initially discussed. According to the Young–Laplace equation, the surface tension of a curved surface is described as

$$\Delta p = \gamma\left(\frac{1}{R_1} + \frac{1}{R_2}\right) \quad (1)$$

where Δp is the pressure difference between the LM droplet and the electrolyte ($\Delta p > 0$) and $1/R_1$ and $1/R_2$ are the principal curvatures for a curved surface. It is known that the surface oxide can severely decrease the surface tension of the droplet.[15,24] When the surface tension (γ) decreases, the pressure difference (Δp) also decreases. Thus, when a certain external force was applied to the droplet, the droplet was easier to deform. This conclusion is also consistent with previous report.[25]

To investigate the mechanism of surface oxide formation, the underlying chemical interactions were analyzed. For the iron particles, part of them only reacts with HCl and generates hydrogen. For the other part of the iron particles, they can interact with gallium physically and chemically. First, the iron particles can be absorbed into gallium, which provide the magnetic property of the MLMD.[3,4] Secondly, when the iron particles were attached to the LM droplet in the HCl solution, galvanic interaction should take place,[4] which is schematically shown in Figure 2a. In details, the standard electrode potentials of Ga, In, and Fe are −0.560, −0.345, and −0.477V, respectively. As Ga has the most negative electrode potentials, it should act as the cathode and lose electrons:

$$Ga - 3e^- \rightarrow Ga^{3+} \quad (2)$$

The iron works as an anode, and the surrounding H^+ received the electrons:

$$2H^+ + 2e^- \rightarrow H_2 \quad (3)$$

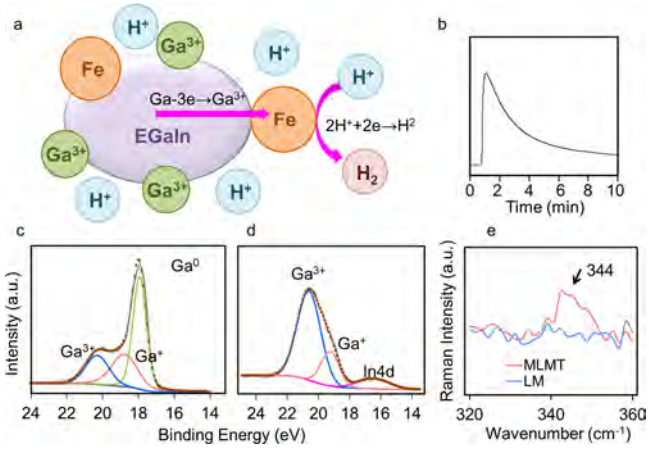

Figure 2. Chemical characterization of the MLMD. (a) Galvanic cells formed between gallium and iron in an acidic solution. The pink arrows indicate the electron flow directions. (b) Gas chromatography of hydrogen gas during the preparation of MLMD. (c) Ga 3d fitted the XPS spectra of LM. (d) Ga 3d fitted XPS spectra of the MLMD. (e) Raman spectrum of the LM (blue) and MLMD (red) in a region of 320–360 cm^{-1}.

H_2 was generated as confirmed by gas chromatography (Figure 2b). In the presence of air, the gallium oxide layer should form on the LM droplet surface. At the same time, the HCl should continuously dissolve the oxide layer. It is supposed that the oxide forming rate facilitated by the galvanic reaction may exceed the dissolving rate of HCl. Thus, gallium oxides formed on the LM droplet surface. To validate this assumption, the surface oxide composition was characterized by X-ray photoelectron spectroscopy (XPS) as well as Raman spectroscopy. For the XPS analysis, the Ga 3d spectra clearly showed the presence of the three chemical states of gallium: the peaks located at 18.1, 19.6, and 20.5 eV were assigned to Ga, Ga_2O, and Ga_2O_3, respectively. For pure LM without iron particles, few Ga_2O and Ga_2O_3 were detected in the droplet surface (Figure 2c). After the addition of iron particles, most of gallium was detected as the Ga^{3+} state, indicating the formation of Ga_2O_3 in abundance (Figure 2d). The Raman spectroscopy also confirmed that the surface oxide was mainly composed of β-Ga_2O_3 as the appearance of a 344 cm^{-1} peak shift[26] (Figure 2e). Thus, it is demonstrated that gallium oxide was formed on the MLMD in the HCl solution. This result also supports the foregoing conclusion that the surface oxide influenced the surface tension of the LM.

The giant deformability of this MLMD can be affected by several factors. For example, more intense galvanic currents should lead to more surface oxide formation. The HCl electrolyte can also play a role by dissolving the surface oxides. To further characterize the MLMD deformation properties, we investigate the influence of several factors on the stretching of MLMD. As it is known that the surface oxide formation should be related with the electrolyte types, different electrolytes were evaluated in influencing the deformability of MLMD. MLMDs with different sizes were transferred into 1 mol/L HCl, 1 mol/L NaCl, 1 mol/L NaOH, or pure water. Then, the stretching properties of MLMD in such electrolytes were measured. The MLMD displayed similar behaviors in NaCl and pure water. As the surrounding solution has no resolving effect, the surface oxide became too thick to maintain the droplet shape. The surface oxide became a paste-like material and stuck to the

DOI: 10.1021/acsami.8b22699
ACS Appl. Mater. Interfaces 2019, 11, 8685–8692

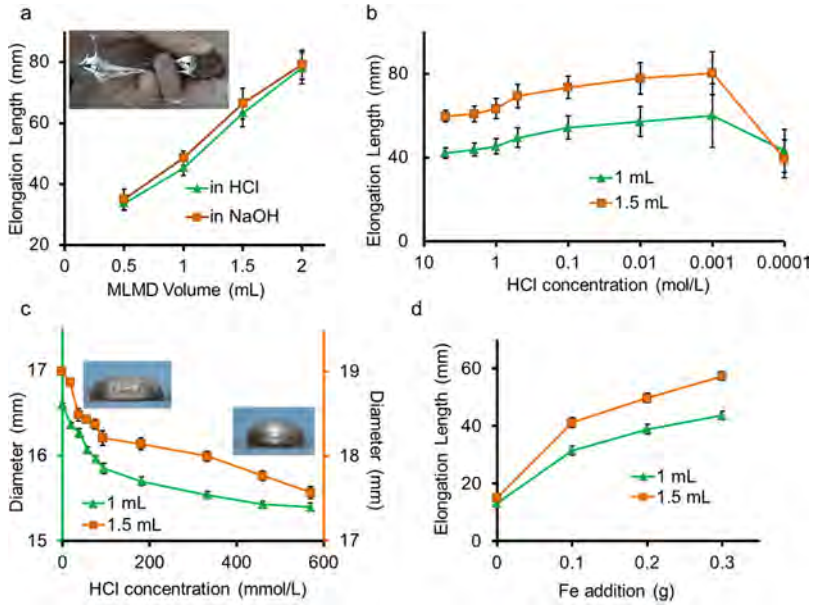

Figure 3. Several factors that may influence the stretching ability of MLMD were evaluated. (a) The largest elongation length of MLMD in different electrolytes including 1 mol/L HCl (green triangle) and 1 mol/L NaOH (orange rectangle). The MLMD became paste-like in 1 mol/L NaCl (inset). (b) The largest elongation length of MLMDs (1 and 1.5 mL) at various HCl concentrations. (c) The diameters of MLMD (1 and 1.5 mL) measured in increasing HCl. The insets are the side views of 1 mL of MLMD in HCl at 0 (deionized water) and 460 mmol/L. (d) The largest elongation length of MLMD when mixing with different amounts of iron.

substrate. The local part of the droplet can be drawn out to a long distance under magnetic control. However, the process was not reversible as the paste-like oxide skin can stick to the substrate. The inset of Figure 3a illustrates an example of paste-like MLMD in NaCl. It should be noted that the galvanic interaction should be relatively weak in water or NaCl. Thus, it should contribute only a small part of the surface oxide, whereas most of which are due to the intrinsic properties of liquid gallium in the presence of air. Meanwhile, in 1 mol/L NaOH, the MLMD can be also stretched into a long stick, which presents similar deformability as that in 1 mol/L HCl (Figure 3a). For droplets with different sizes, their deformation showed no significant difference. The chemical interaction taking place in NaOH was also investigated. For gallium, it can also react with NaOH and produce hydrogen because of its amphotericity.[4] Gallium can also form a galvanic cell with iron, which should also enhance the surface oxide formation in the presence of air.[13] Thus, the surface tension of the MLMD was also reduced in NaOH and can be stretched in the NaOH solution to such a large degree. The whole results suggest that the surface oxide with proper thickness is the key for the reversible stretching deformation of the MLMD.

As the chemical and physical properties of the droplet surface seem to play an important role in determining its surface tension as well as the deformability, other factors that may affect the surface properties were further studied. To evaluate the deformability of MLMD, the largest elongation length was measured. We define the largest elongation length of MLMD as the length of stretching MLMD right before it breaks into two parts (tensile failure). Figure 3b illustrates how the HCl concentration affects the stretching ability of the MLMD. The result suggests that when the HCl concentration decreases, the MLMD can be further stretched, which indicates the improvement of deformability. On the basis of the observation, the droplet was brighter in HCl at higher concentrations, which implied less surface oxide and higher surface tension over the droplet. This result is consistent with our previous conclusion that HCl can dissolve surface oxide and increase surface tension of the LM droplet. As the HCl concentration decreased, the droplet became more oxidized. The continuously forming oxide can impede the reversible transformation of the MLMD from a droplet to a long-stick shape. Thus, the elongated length also became more affected, which can be also reflected in the growing error bars. It is noteworthy that when the HCl concentration is lower than 10^{-4} mol/L, the dissolving effect of HCl seemed too weak. Thus, the MLMD became severely oxidized, and tensile failures often occur (Figure S1 in Supporting Information). We also examine the droplet morphology in relation to the HCl concentration. The MLMD was placed in 10 mL of deionized water at first. Then, a certain volume of HCl was gradually and gently added into the water. After 2 min, HCl was supposed to be uniform in the solution, and the diameter of the MLMD was measured. This process was repeated 10 times (five times addition of 100 μL of 2 mol/L HCl followed by another five times of 500 μL of 2 mol/L HCl in sequence). The diameters as well as the side-view images of the MLMDs (1 and 1.5 mL) suggest that when the HCl concentration increased, the droplet became contracted with a shorter diameter, which also supported the increasing surface tension (Figure 3c). It should be noted that although the increasing HCl concentration can enhance the galvanic effects and further facilitate the oxidation of gallium, the dissolving effect of HCl at high concentrations also increased. Thus, the MLMD has a lower surface tension when HCl concentration is higher.

In another experiment, we also evaluate on how the iron particles affect its stretchability. It is supposed that more iron particles attached to the LM droplet surface will lead to more intense galvanic reaction, which will enhance the formation of surface oxide and more surface oxide can lead to a higher stretchability, that is, elongation length in this study. To confirm this, relative experiments are designed and carried out

DOI: 10.1021/acsami.8b22699
ACS Appl. Mater. Interfaces 2019, 11, 8685−8692

as below. Different amounts of iron particles were added to the LM to prepare various MLMDs with different amounts of iron particles. Those MLMDs were then transferred into clean 1 mol/L HCl again for the elongation measurement by magnetic manipulation. This process was repeated three times, and the elongation of the MLMD was characterized. The results shown in Figure 3d also suggest that more iron particles in the MLMD can lead to the longer elongation length of the MLMD. This result also supports our assumption that more iron particles in the MLMD lead to better stretchability.

It has been reported that the LM droplet containing a small amount of iron particles can be manipulated by magnetic fields.[3] These studies took advantages of the deformable body of the LM droplet and manipulated it in microfluidic channels. However, the droplet can only move as a whole without such large and complex deformation in the open space. The ability of reversible elongation in such large extend for the conductive MLMD is undoubtedly desirable for functional development in the design of future soft devices. To further characterize this elongation, the force analysis was carried out. In the present study, when the magnetic field was applied to the droplet, the iron particles in the MLMD were attracted to and moved along with the magnets. Thus, it provided a force that elongates the MLMD. We modeled the elongated LM stick as a cylinder coated with a thin shell of surface oxide with uniform thickness. The tensile force can be approximated using the eq 4, where F is the applied force, r is the minimum radius of the LM stick, and σ is the tensile surface yield stress:

$$F = 2\pi r\sigma \quad (4)$$

In this model, the applied force is not easy to measure because the attraction between two magnets is so high that significantly interfere the force measurement. We consider that the surface tension generally maintains the same during the elongation. Then, we measure the interfacial tension across the MLMD and 2 mol/L HCl in the statistic state using a surface tension meter DCAT11 (Dataphysics, Germany). The measured surface tension is 302.7 ± 11.4 (n = 30) mN/m, which is similar to the previously reported value of the critical surface yield stress of the oxide (~0.5 N/m) measured in shear.[28] This measured surface tension may be also affected by the iron particles that spread on the oxide skin. For a 1.5 mL of MLMD, the minimum radius of the LM sticks is around 0.65 ± 0.13 mm. Thus, the applied force provided by magnetism should be around 1.25 mN along the elongation direction. Compared with other stretchable and conductive materials,[25] the applied force required for stretching this MLMD is quite small, whereas the stretchability can reach 400%, which present great value in some applications such as intelligent circuits or devices.

Figure 4 illustrates a conceptual experiment in which MLMD worked as an intelligent scalable conductor (Movie S4 in Supporting Information). In the space of a hexagonal plane (each side length is 30 mm), 1 mL of MLMD was placed in 10^{-3} mol/L HCl in this example. Although the HCl concentration is relatively low, it is still a strong electrolyte in which a weak current can pass through. Thus, at the original state, the bulbs can give off faint light. Under the manipulation of a magnet, the MLMD can be stretched and swerved to connect certain two ports of the circuits. Then, the LED bulbs were completely lighted up. In this case, the MLMD presents good deformability and stretchability, which is a promising candidate material for flexible and stretchable device design.

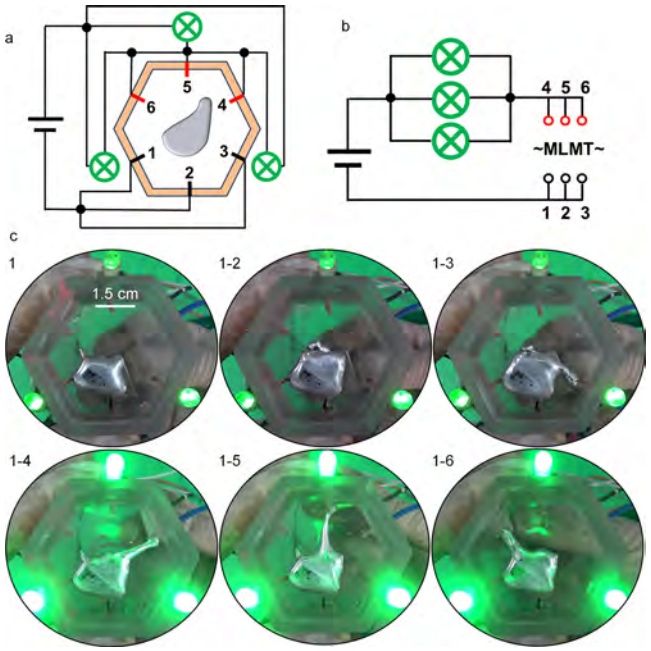

Figure 4. Conceptual experiment in which MLMD worked as an intellectual scalable conductor. (a) The schematic illustration of the experimental design. (b) The simplified circuit diagram of (a). (c) The bulbs were dim when the MLMD connected negative ports (1, 1−2, 1−3). When the MLMD connected one positive and one negative ports (1−4, 1−5, 1−6), the bulbs were completely lighted up.

Moreover, the local part of the droplet can be precisely and conveniently manipulated by the magnetic field, which shed light on intelligent soft robot design and control in the future.

In the above results, the MLMD have displayed multi-degrees of freedom in the horizontal plane, which already showed great potential for some applications such as intelligent scalable circuits. For further development of the functions of MLMD, it would be pursued if the MLMD can be manipulated in the three-dimensional space. For this reason, we investigated the stretchable deformability of MLMD in the vertical direction. The experimental device is illustrated in Figure 5a. A transparent plastic box with a cap was utilized in this study. Two electrodes connecting to an LED bulb were fixed on the ceiling and bottom of the box, respectively, at a distance of around 3 cm. When two magnets were applied on the top of the box (around 3 cm above the droplet), a small part of the MLMD can be attracted to touch the ceiling of box because of the magnetic attraction. Surprisingly, the MLMD can connect the two electrodes on the top and the bottom through a narrow wire-like part. The lighted-up green bulb also proved that the two electrodes were successfully connected (Figure 5b and Movie S5 in Supporting Information). The diameter of the narrowest part is around 0.8 to 1.2 mm. This vertically stretching state can last several seconds before any mechanical disturbance. In the example in Movie S5, it last at least 8 s before we took the initiative to break the connection. More intriguingly, the electrode on the top was above the liquid level. Thus, the top part of the MLMD was directly exposed to the air while maintaining standing. When the magnets were removed, the upper part dropped into the HCl solution and became a liquid droplet again. The standing process can be less than 0.5 s. This process can be repeated at least 50 times for one MLMD.

DOI: 10.1021/acsami.8b22699
ACS Appl. Mater. Interfaces 2019, 11, 8685−8692

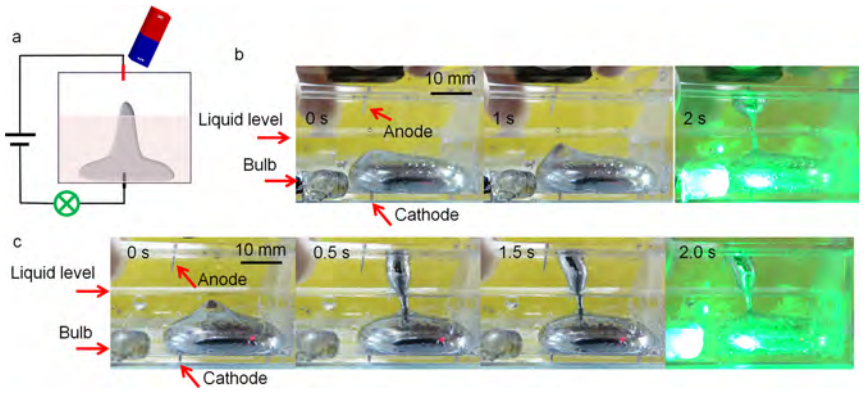

Figure 5. MLMD can stretch and move in the vertical direction. (a) The schematic diagram of the experimental settings. (b) The MLMD can quickly stretch in the vertical direction and connect the anode and the cathode to light up the bulb. (c) The vertically stretched MLMD can move horizontally to connect two electrodes to light up the bulb.

On the basis of our preliminary study, the intensity of magnetic fields also influences this vertical elongation behavior. When low magnetic field intensity (one magnet only, around 50 G at a distance of 30 mm right above the droplet) was applied, the iron particles in MLMD cannot be attracted to the ceiling of the box. Thus, the MLMD cannot stand up as we desire. When a high magnetic field intensity (four magnets together, around 220 G at a distance of 30 mm) was applied, the vertical stretching behavior can be also observed (Figure S2 in Supporting Information). This result implies generally that a higher magnetic field intensity is preferred for the vertical stretching behavior of MLMD. It should be noted that the high magnetic field can provide a large magnetic attraction. Thus, part of the MLMD will rush at the top at a relatively high speed. When it reached the ceiling of the box, the quick hit may bring a considerable mechanic shock to the whole MLMD, which sometimes easily break the narrow part of the MLMD. To acquire stable performance of such vertical stretching behavior, more sophisticated magnetic manipulation requires to be developed.

To further improve the function of this MLMD, the planar motion was explored. After MLMD was connecting the top and bottom pulled by the magnetic field, the magnets were slowly moved horizontally. It was observed that the MLMD also moved with the magnets while remained up and down connected. A conceptual experiment illustrated this behavior (Figure 5c and Movie S6 in Supporting Information). The standing MLMD moved from a distance at around 10 mm to the top electrode. Then, the bulb was lighted up, indicating the two electrodes were connected by the MLMD. On the basis of our observation, during the move of the top part, the bottom part of the MLMD had a little displacement. The connecting long thin cylinder part in the middle also leaned with the top. As the oxide surface has certain stiffness, the top and middle parts of MLMD as a whole can be modeled as a cantilever beam. When given a horizontal displacement at the top end, the deformation pattern of the middle part is analogous to a cantilever beam subjected to an end displacement. However, as the MLMD also has the physical property of the liquid, the deformation is slightly different from a stiff beam. The moving speed of top end can reach around 5.4 mm/s with up and down connected. When the speed became too high, the connection was easy to break. It is noteworthy that part of the MLMD was immersed in the liquid, whereas the other part was exposed in the air. Thus, the whole process of MLMD showed great resemblance to the behavior of an amphibian, which is striking and inspiring.

Such behavior of the MLMD in the vertical direction is inspiring. Compared with the statically standing liquid metal microstructures in previous report,[29] the MLMD exhibits great advancement for several aspects. First, the stretching length of the MLMD in the vertical direction can be at least 3 cm, which is far more than the tallest free standing liquid metal structure (~1 cm). Besides, this standing behavior of MLMD is reversible and repeatable for multiple times. Most surprisingly, the standing MLMD can also move, which behaves more like a functional robot. In the present study, the MLMD can stand up in the vertical direction in almost totally open space without external support from the other structures. Under the control of the magnets, this behavior can be easily and precisely achieved without any external electrical devices, which is quite simple and convenient. All these behaviors of MLMD exhibited great potential and value for future soft robot design.

CONCLUSIONS

In summary, this study presents a multimaterials-based magnetic liquid metal droplet, which owns the abilities of quick and reversible stretching and moving in large scales. The stretching behavior can be achieved in the three dimensions of the totally free open space. The surface oxide over the MLMD body plays the key role in enhancing its deformability as well as the mechanical strength for this 3D stretch. With those intriguing abilities, this MLMD can work as an intelligent scalable conductor to make electrical switches, which can be regulated exactly from point to point in the three-dimensional space. The vertically stretched MLMD can even move horizontally with its half body in the solution and the other half in the air, which quite resembles the nature of an upright walking amphibian. As the MLMD is highly deformable, it may be applied in more complex circumstances for further development. In addition, all those behaviors can be precisely and conveniently controlled by the magnetic field provided by permanent magnets, which is promising for future soft robot design and fabrication. Above all, with such ubiquitous and valuable properties and abilities, the MLMD in the present study may provide a platform for the further development of liquid metals in the intelligent soft robot with more sophisticated functions in the free and open space.

DOI: 10.1021/acsami.8b22699
ACS Appl. Mater. Interfaces 2019, 11, 8685−8692

EXPERIMENTAL SECTION

MLMD Preparation and Manipulation. The preparation process of MLMD has been introduced in the Result section. Here, we introduce the preparation of a liquid metal. All the liquid metal (LM) droplets used in the experiments were GaInSn alloy prepared from gallium, indium, and tin with a purity of 99.99%. These raw materials with mass ratios of 67:12:13, respectively, were added into a beaker and then heated to 100 °C. A magnetic stirrer was used to stir the mixture uniformly after the metals were all melted. All the HCl and NaOH electrolytes used in this study were freshly made before the experiments. The iron particles with a diameter from 50 to 100 μm were purchased from DK Nano Technology. The magnetic field is provided by neodymium iron boron magnets. Then, the dynamic motion of MLMD was observed and recorded by digital video equipment, Sony HDR-PJ670.

Surface Tension Measurement. In this study, the surface tension generally indicates the interfacial tension between the LM droplet and surrounding liquids unless otherwise specified. The interfacial tension of MLMD in 2 mol/L HCl was determined by a surface tension meter DCAT11 (Dataphysics, Germany). Briefly, the surface tension of HCl (relatively low surface tension) and MLMD (relatively high surface tension) was measured successively and respectively. Then, the interfacial tension of MLMD and HCl was measured. Thus, the surface tension of the MLMD in HCl was determined.

Surface Oxide Composition Characterization. The surface composition of MLMD was examined by X-ray photoelectron spectroscopy. The results were analyzed using XPSPEAK41. A Raman microscope (inVia-Reflex, Renishaw) was also used to determine the composition of surface oxide with a 532 nm laser as the excitation source. A 10× objective lens is used to focus the excitation laser and to collect Raman spectra in back reflection.

ASSOCIATED CONTENT

Supporting Information

The Supporting Information is available free of charge on the ACS Publications website at DOI: 10.1021/acsami.8b22699.

Further description of the MLMD stretching in extreme low HCl and under relatively high magnetic field (PDF)

Stretching of MLMD (AVI)

Reversibility and repeatability (AVI)

Local manipulation (AVI)

Intellectual scalable conductor (AVI)

Vertically stretch (AVI)

Up-right walking (AVI)

AUTHOR INFORMATION

Corresponding Authors

*E-mail: cnhuliang@buaa.edu.cn (L.H.).
*E-mail: jliu@mail.ipc.cn.cn (J.L.).

ORCID

Liang Hu: 0000-0003-1648-7696
Hongzhang Wang: 0000-0003-2733-9461
Jing Liu: 0000-0002-0844-5296

Notes

The authors declare no competing financial interest.

ACKNOWLEDGMENTS

This work is supported by the 111 Project (Project No.B13003) and the National Natural Science Foundation of China (Grant No.81801794).

REFERENCES

(1) Tang, S.-Y.; Khoshmanesh, K.; Sivan, V.; Petersen, P.; O'Mullane, A. P.; Abbott, D.; Mitchell, A.; Kalantar-zadeh, K. Liquid Metal Enabled Pump. *Proc. Natl. Acad. Sci. U. S. A.* **2014**, *111*, 3304−3309.

(2) Gao, M.; Gui, L. A Handy Liquid Metal Based Electroosmotic Flow Pump. *Lab Chip* **2014**, *14*, 1866−1872.

(3) Jeon, J.; Lee, J.-B.; Chung, S. K.; Kim, D. On-Demand Magnetic Manipulation of Liquid Metal in Microfluidic Channels for Electrical Switching Applications. *Lab Chip* **2016**, *17*, 128−133.

(4) Wang, H.; Yuan, B.; Liang, S.; Guo, R.; Rao, W.; Wang, X.; Chang, H.; Ding, Y.; Liu, J.; Wang, L. PLUS-M: A Porous Liquid-Metal Enabled Ubiquitous Soft Material. *Mater. Horiz.* **2018**, *5*, 222−229.

(5) Zhang, J.; Yao, Y.; Sheng, L.; Liu, J. Self-Fueled Biomimetic Liquid Metal Mollusk. *Adv. Mater.* **2015**, *27*, 2648−2655.

(6) Tang, S.-Y.; Sivan, V.; Petersen, P.; Zhang, W.; Morrison, P. D.; Kalantar-zadeh, K.; Mitchell, A.; Khoshmanesh, K. Liquid Metal Actuator for Inducing Chaotic Advection. *Adv. Funct. Mater.* **2014**, *24*, 5851−5858.

(7) Russell, L.; Wissman, J.; Majidi, C. Liquid Metal Actuator Driven by Electrochemical Manipulation of Surface Tension. *Appl. Phys. Lett.* **2017**, *111*, 254101.

(8) Chrimes, A. F.; Berean, K. J.; Mitchell, A.; Rosengarten, G.; Kalantar-zadeh, K. Controlled Electrochemical Deformation of Liquid-Phase Gallium. *ACS Appl. Mater. Interfaces* **2016**, *8*, 3833−3839.

(9) Sheng, L.; Zhang, J.; Liu, J. Diverse Transformations of Liquid Metals between Different Morphologies. *Adv. Mater.* **2014**, *26*, 6036−6042.

(10) Tan, S.-C.; Yuan, B.; Liu, J. Electrical Method to Control the Running Direction and Speed of Self-powered Tiny Liquid Metal Motors. *Proc. R. Soc. A* **2015**, *471*, 20150297.

(11) Zhang, J.; Guo, R.; Liu, J. Self-propelled Liquid Metal Motors Steered by a Magnetic or Electrical Field for Drug Delivery. *J. Mater. Chem. B* **2016**, *4*, 5349−5357.

(12) Zavabeti, A.; Daeneke, T.; Chrimes, A. F.; O'Mullane, A. P.; Ou, J. Z.; Mitchell, A.; Khoshmanesh, K.; Kalantar-Zadeh, K. Ionic Imbalance Induced Self-Propulsion of Liquid Metals. *Nat. Commun.* **2016**, *7*, 12402.

(13) Chechetka, S. A.; Yu, Y.; Zhen, X.; Pramanik, M.; Pu, K.; Miyako, E. Light-Driven Liquid Metal Nanotransformers for Biomedical Theranostics. *Nat. Commun.* **2017**, *8*, 15432.

(14) Yu, Y.; Miyako, E. Manipulation of Biomolecule-Modified Liquid-Metal Blobs. *Angew. Chem.* **2017**, *56*, 13606−13611.

(15) Hu, L.; Wang, L.; Ding, Y.; Zhan, S.; Liu, J. Manipulation of Liquid Metals on a Graphite Surface. *Adv. Mater.* **2016**, *28*, 9210−9217.

(16) Yu, Y.; Miyako, E. Alternating-Magnetic-Field-Mediated Wireless Manipulations of a Liquid Metal for Therapeutic Bioengineering. *iScience* **2018**, *3*, 134−148.

(17) Xiong, M.; Gao, Y.; Liu, J. Fabrication of Magnetic Nano Liquid Metal Fluid through Loading of Ni Nanoparticles into Gallium or Its Alloy. *J. Magn. Magn. Mater.* **2014**, *354*, 279−283.

(18) Guo, R.; Wang, X.; Chang, H.; Yu, W.; Liang, S.; Rao, W.; Liu, J. Ni-GaIn Amalgams Enabled Rapid and Customizable Fabrication of Wearable and Wireless Healthcare Electronics. *Adv. Eng. Mater.* **2018**, *20*, 1800054.

(19) Daalkhaijav, U.; Yirmibesoglu, O. D.; Walker, S.; Mengüç, Y. Rheological Modification of Liquid Metal for Additive Manufacturing of Stretchable Electronics. *Adv. Mater. Technol.* **2018**, *3*, 1700351.

(20) Jeon, J.; Lee, J.-B.; Sang, K. C.; Kim, D. In Magnetic Liquid Metal Marble: Wireless Manipulation of Liquid Metal Droplet for Electrical Switching Applications, *18th International Conference on Solid-State Sensors, Actuators and Microsystems (TRANSDUCERS)*, Anchorage, AK, June 21−25, 2015; IEEE: Piscataway, NJ, 2015; pp 1834−1837.

DOI: 10.1021/acsami.8b22699
ACS Appl. Mater. Interfaces 2019, 11, 8685−8692

(21) Carle, F.; Bai, K.; Casara, J.; Vanderlick, K.; Brown, E. Development of Magnetic Liquid Metal Suspensions for Magneto-hydrodynamics. *Phys. Rev. Fluids* **2017**, *2*, 013301.
(22) de Castro, I. A.; Chrimes, A. F.; Zavabeti, A.; Berean, K. J.; Carey, B. J.; Zhuang, J.; Du, Y.; Dou, S. X.; Suzuki, K.; Shanks, R. A.; Nixon-Luke, R.; Bryan, G.; Khoshmanesh, K.; Kalantar-zadeh, K.; Daeneke, T. A Gallium-Based Magnetocaloric Liquid Metal Ferrofluid. *Nano Lett.* **2017**, *17*, 7831−7838.
(23) Hu, L.; Li, J.; Tang, J.; Liu, J. Surface Effects of Liquid Metal Amoeba. *Sci. Bull.* **2017**, *62*, 700−706.
(24) Khan, M. R.; Eaker, C. B.; Bowden, E. F.; Dickey, M. D. Giant and Switchable Surface Activity of Liquid Metal via Surface Oxidation. *Proc. Natl. Acad. Sci. U. S. A.* **2014**, *111*, 14047−14051.
(25) Hu, L.; Yuan, B.; Liu, J. Liquid Metal Amoeba with Spontaneous Pseudopodia Formation and Motion Capability. *Sci. Rep.* **2017**, *7*, 7256.
(26) Rao, R.; Rao, A. M.; Xu, B.; Dong, J.; Sharma, S.; Sunkara, M. K. Blueshifted Raman Scattering and its Correlation with the [110] Growth Direction in Gallium Oxide Nanowires. *J. Appl. Phys.* **2005**, *98*, 094312.
(27) Zheng, Y.; He, Z.; Gao, Y.; Liu, J. Direct Desktop Printed-Circuits-on-Paper Flexible Electronics. *Sci. Rep.* **2013**, *3*, 1786.
(28) Yu, Y.; Zeng, J.; Chen, C.; Xie, Z.; Guo, R.; Liu, Z.; Zhou, X.; Yang, Y.; Zheng, Z. Three-Dimensional Compressible and Stretchable Conductive Composites. *Adv. Mater.* **2014**, *26*, 810−815.
(29) Ladd, C.; So, J.-H.; Muth, J.; Dickey, M. D. 3D Printing of Free Standing Liquid Metal Microstructures. *Adv. Mater.* **2013**, *25*, 5081−5085.

DOI: 10.1021/acsami.8b22699
ACS Appl. Mater. Interfaces 2019, 11, 8685−8692